Impact of physical constraints on the dynamical properties of neuronal networks

Author: Marc Pielies Avellí
Facultat de Física, Universitat de Barcelona, Diagonal 645, 08028 Barcelona, Spain.

Advisor: Dr. Jordi Soriano Fradera
Departament de Física de la matèria condensada.

Abstract: The spatial arrangement of the neurons conforming a neuronal network exerts a crucial influence on the activity patterns exhibited by the ensemble. But how exactly this dependence is manifested and in which ways it can be parametrized is still a matter of debate. To advance in this quest, in this work we analyze a number of cultures grown in differently patterned surfaces. We consider a substrate with 4 deep cavities and a substrate with mild topographical modulation on its surface. The results show that the 4 cavities shape a weakly connected set of cultures which altogether shape a very rich dynamics with clear modularity, traits that are much weaker in the other culture. Altogether, the results show the interest but difficulty of making tailored circuits with simple topographical constraints.

I. INTRODUCTION

The relation between the functional connectivity of a neuronal circuit and the structural configuration of the network from which the first one arises constitutes a fundamental paradigm in neuroscience still to be well understood. Due to the sheer size of the brain, scientists have found in *in vitro* cortical cultures a new framework to analyze neuronal systems as a whole while being able to distinguish individual neurons. In such a controlled environment, small perturbations can be applied into the relief of the substrates in which neurons grow in order to quantify and compare the changes in the dynamical response of the cultures.

A number of strategies have already proved to be useful when trying to relate certain activity patterns to specific structural attributes of the networks. For instance, *Okujeni et al.* [1] adjusted the physical distribution of neuronal networks by pharmacological modulation of protein kinase C (PKC), an enzyme which regulates neurite growth. With a similar goal, *Yamamoto et al.* [2] focused their research on cultures with differently bounded modules grown in micropatterned substrates. As we will see, the results of this work are in deep agreement with the ones obtained by the former investigators.

II. EXPERIMENTAL METHODS

***In vitro* cultures.**— The experimental procedure begins with the procurement of primary cortical neurons from the brain of a rat embryo. Once the brain is dissected, dissociated neurons are suspended in a proper medium and plated into a polydimethylsiloxane (PDMS) mold, where they develop new connections.

This apparently naive step of the method underlies one of the most important advantages of the *in vitro* technique: since these cultures are created from scratch, neurons do not display any kind of 'structural memory' so the dynamical traits of the culture will be genuinely influenced by the characteristics of the physical support where they grow, which can be modeled by means of physical obstacles or traps.

After $5-7$ days *in vitro* (DIV), neurons start to fire in a collective manner if they receive a number of stimuli over a threshold in a non-linear activated process, which arises from the system's noise together with amplification of activity towards nucleation regions, as described in [3].

Neuronal firings within a collective activity episode propagate through the neuronal axons in the form of potential differences mediated by Ca^{2+} ions, giving rise to quasi-periodical *network bursts* that typically involve a large fraction of the neurons in the network. Activity propagation can be recorded with high spatio-temporal resolution using Calcium fluorescence imaging, recordings with which we will be able to evaluate the widely varied activity patterns of our neuronal networks.

Calcium imaging and detection of spikes.— To track the activity of the cells, they are infected using a virus with Genetically-Encoded Calcium Indicators (GECI's). Calcium indicators are based on ultrasensitive fluorescence protein calcium sensors (such as GCaMP6), which cause a significant increase in brightness when a change in their conformation takes place due to the binding between the protein and Ca^{2+} ions.

Fluorescence recordings are thereupon processed using the tool NETCAL [4], a software from Soriano's lab that provides the pipeline to extract traces related to the relative fluorescence of Regions Of Interest (ROIs) over the images and are associated with neurons (Figs. 1A-B).

From fluorescence data one extracts the *spike* of a neuron, i.e. an activity event. We used the Schmidt trigger to infer these spikes: whenever the fluorescence signal passes a first high threshold and remains above a second lower one for a given time, a spike is assumed to occur (Fig. 1C). This method permits the characterization of the collective behaviour of the neuronal network (visualizing it as raster plots, Fig. 2A-CI), while discarding neuronal reverberance phenomena and noise artifacts.

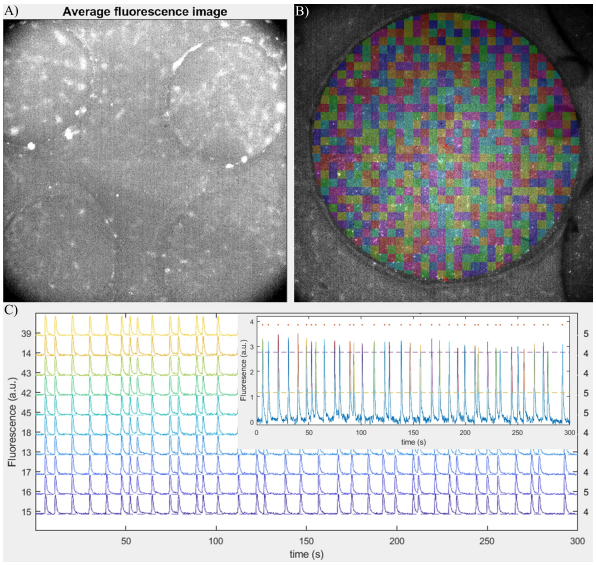

FIG. 1: a) Fluorescence image of a neuronal culture. b) ROIs detected with a circular grid. c) Smoothed traces and spike inference using the Schmidt trigger method.

III. DATA ANALYSIS METHODS

The raw output of NETCAL contains a list of ROIs together with the time when their spikes were detected. Hence, to extract quantifiable information about our network's properties, several mathematical tools must be introduced:

Correlation coefficients.— Pairwise Pearson correlation coefficients provide a first overview of functional communication between neurons i and j. The correlation coefficient r is given by

$$r_{ij} = \frac{\sum_t [x_i(t) - \overline{x}_i]\,[x_j(t) - \overline{x}_j]}{\sqrt{\sum_t [x_i(t) - \overline{x}_i]^2}\sqrt{\sum_t [x_j(t) - \overline{x}_j]^2}}. \quad (1)$$

However, this parameter is strongly influenced by time discretization: causally related events delayed even a single time frame are not taken into account. Moreover, spurious correlations cannot be detected: if two neurons are stimulated by a third one, the first couple will appear to be connected, which possibly may not be the case.

Transfer Entropy and Z-score.— To correctly evaluate *causal* relations and time delays it is opportune to introduce Transfer Entropy (TE) in our toolbox, a [0,1] bounded measure aimed to quantify the amount of transferred information between neurons. Thus, TE values close to 0 are related to fully random or fully synchronous states of the system, while a value near to 1 indicates substantial influence of a neuron onto another.

TE provides functional connections. It is convenient to define a cutting threshold to set the significance of these connections, excluding those that can occur randomly. This is normally done by assuming that TE scores that substantially deviate from the mean $\langle \mathrm{TE} \rangle$ are the most reliable. This is implemented with a Z-score, which sets the strength of a functional connection as standard deviation units from the mean $\langle \mathrm{TE} \rangle$. Based from experience in Soriano's lab, a Z-score of 0.1 reflects functional connections that belong to collective synchronous events, i.e. provides a similar measure as correlation but with lower spurious connections. Under this conditions, this is how we obtained the adjacency matrix of functional connections.

Global network activity (GNA).— Global network activity distributions are probability distribution functions of the fraction of neurons involved in network bursts. A lower limit is set to 5% of the neurons of the culture in order to remove sporadic and random bursts.

Functional complexity and dynamical richness.— Following [2] and [5], the functional complexity of a magnitude assigns a numerical value to the variability of possible states in which the given magnitude can be found. For our study, Θ_{CC} and Θ_{GNA}, which stand for the variability among the activity patterns of firing neurons and the variability among the number of neurons involved in GNAs, respectively, will be specially relevant. By multiplying both of them we obtain the 'dynamical richness' of the network, an indicator that takes values ranging from 0 to 1:

$$\Theta = \Theta_{\mathrm{CC}}\Theta_{\mathrm{GNA}} =$$

$$\left(1 - \tfrac{m}{2(m-1)} \sum_{\mu=1}^{m} \left|p_\mu(r_{ij}) - \tfrac{1}{m}\right|\right)\left(1 - \tfrac{m}{2(m-1)} \sum_{\mu=1}^{m} \left|p_\mu(\Gamma_t) - \tfrac{1}{m}\right|\right) \quad (2)$$

In Θ, the value 0 is associated to fully synchronous or fully random activity states of the system. At the oher extreme, Θ values close to 1 are related to uniform distributions of correlation coefficients and GNA values: a perfectly weighted combination of contributions in the entire range of possible values for each variable.

Community detection.— To translate into a numerical value the strength of the divisions of a network into modules, a useful parameter is the *modularity* $\mathcal{Q}$. $\mathcal{Q}$ values close to 1 indicate that neurons tend to functionally connect in distinct groups or modules, and with few interaction among modules. A value close to 0 indicates that all neurons functionally connect to one another similarly, as in a random graph.

Global efficiency.— A last scalar that has to be introduced concerns the easiness of communication between pairs of neurons. This parameter, at the end, quantifies the integration capacity of our neuronal network and is directly related to shortest path distances connecting nodes. As it is done in Refs. [2] and [6], Global

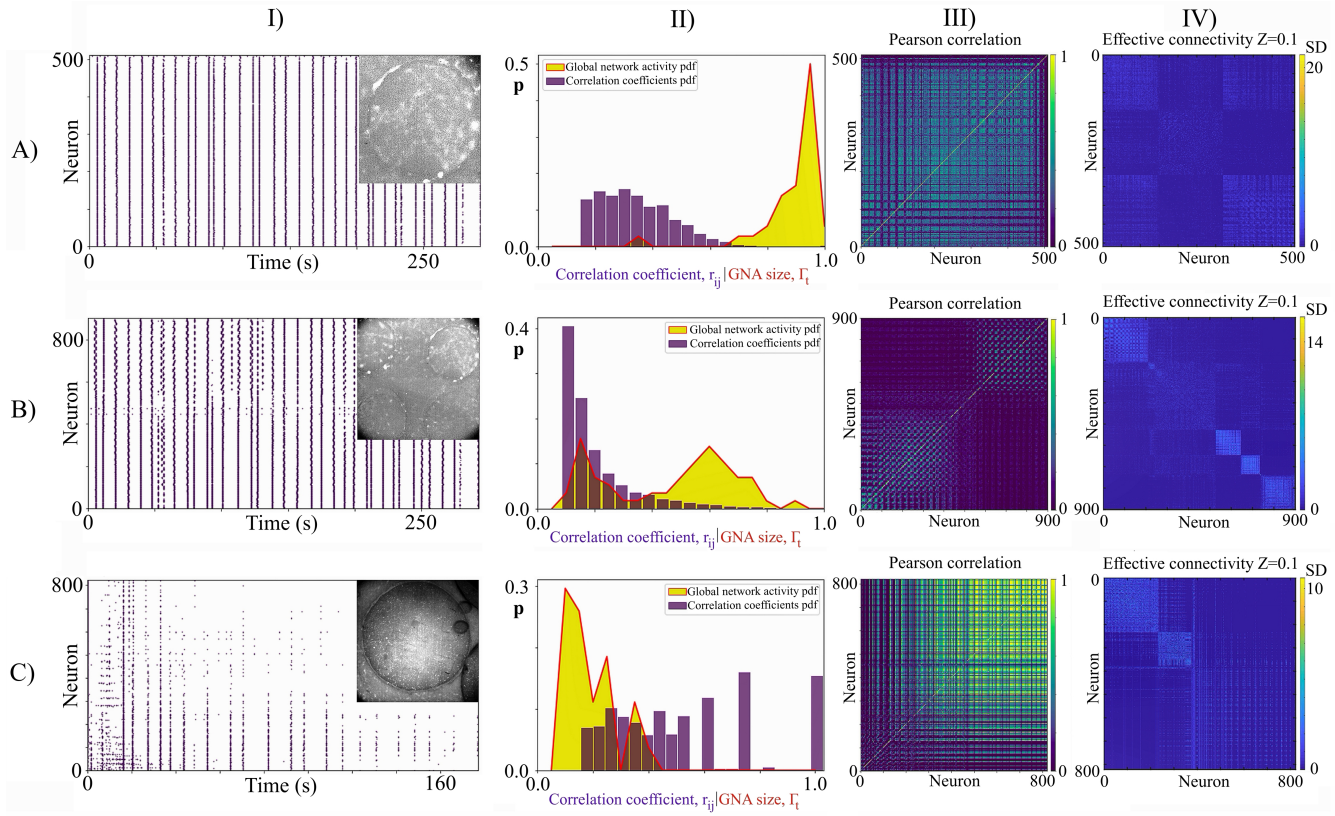

FIG. 2: Summary of the obtained results for each studied culture. From top to bottom we have: a) the homogeneous culture, b) the 4-moduled culture and c) the culture in an embossed PDMS substrate. From left to right we can observe: I) the raster plot of the spikes detected for each neuron, II) probability distribution functions for both pairwise Pearson correlation coefficients (CCs) and global network activations (GNAs), from which we can calculate the functional complexity and dynamical richness of the culture, III) the connectivity matrix weighted using CC values and IV) the connectivity matrix weighted using TE values and a Z-score $Z = 0.1$.

efficiency can be calculated as:

$$G_{\text{EFF}} = \frac{1}{N(N-1)} \sum_{j \neq i} d_{ij}^{-1}, \tag{3}$$

where d_{ij} denotes the shortest path length or minimum topological distance between neurons i and j.

IV. RESULTS AND DISCUSSION

A. A homogeneous culture

As an example of the simplest system of study, a homogeneous culture where 509 ROIs were detected was recorded for 300 seconds at 20 fps. By focusing on the raster plot of the firings (Fig. 2AI) the first thing that must be emphasized is a more than notorious synchronization of the whole network. Quasi-periodical bursts every roughly 10 s are evinced in the second graph, where a sharp peak corresponding to whole network bursts dominates the GNA distribution (Fig. 2AII).

With regard to cross-correlation values, a first overview of their distribution (Fig. 2AIII) does not provide much information, since our time discretization has shifted and smoothed the sharp peak at $r = 1$ limit that intuitively should be expected for full synchronization.

Note that a lower threshold, calculated using surrogates for each culture, has been introduced for CC distributions. Surrogates consisted on randomized time series of firing events, which maintained the total number of spikes per neuron constant but erased any temporal correlation between them. The average value of CCs was then set as a lower limit for the parameter, in this particular case being $\langle \text{CC} \rangle \simeq 0.12$.

In spite of this fruitless first attempt, with a more detailed perusal of the data we can bring to light the main properties of this kind of cultures: looking at the third graph, corresponding to the adjacency matrix from CC, it is evident that there are no privileged modules: all ROIs are similarly connected to each other, with no preferential attachment to a reduced group of them which would be translated into brighter islands on top of the diagonal of the matrix. Besides, the matrix obtained from TE analysis is similar to CC and provides for this case a similar information, i.e. that neurons talk to one another as a uniform, coherent system.

These facts are highlighted by: (1) a high global efficiency $G_{\text{EFF}} \simeq 0.91$, illustrating a highly connected network; (2) a very small $\mathcal{Q}$ value of $\mathcal{Q} \simeq 0.08$, meaning that this huge connected component can be understood as a single community; and (3) a poor dynamical richness of $\Theta \simeq 0.09$, as synchronous states are thoroughly predictable and therefore the palette of available activity patterns for the network is scarce.

B. 4 interconnected homogeneous cultures

The prior scenario changes significantly when a zoom out is performed. Four weakly interconnected homogeneous cultures are studied and recorded simultaneously with the same settings as before. Each culture grows in the wells of a PDMS mold (Fig. 1A). The culture studied above corresponds to one of them. Albeit the behaviour of the neurons within each well can be described in the same manner as it was formerly done, interlinked activity patterns emerge from the combination of the four wells.

Even though the interburst intervals (IBIs) remain the same, the raster plot seems to be segmented into distinguishable blocks. In addition, GNA sizes are now much better distributed across the range of possible values, with a peak near two thirds of the network and another one for bursts involving a little less than 20% of the culture's ROIs (Fig. 3).

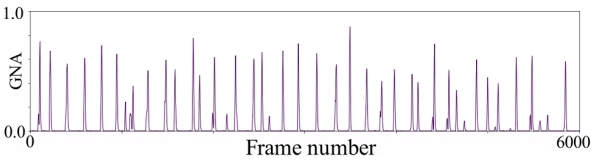

FIG. 3: GNA windowed evolution for the 4-well culture.

CCs distribution in Fig. 2-BII is clearly not in agreement to what we see in the raster, as columns of bursts can be observed neatly. However, as the criteria applied is shared among all cultures, the shift to the left of the distribution could be possibly attributed to a higher difficulty of the neurons to communicate with each other, as time delays between causally related firings are now more pronounced than before.

This hypothesis is further confirmed with a fall in global efficiency's value to $G_{\text{EFF}} \simeq 0.74$, although it is still remarkable; and a considerably increased $\mathcal{Q}$ value of $\mathcal{Q} \simeq 0.37$, which is obtained from the adjacency matrix using Pearson's values as weights of the links (Fig. 2-BIII).

If we opt for studying the adjacency matrix obtained from TE values, the tendency to show towering modularities is also reinforced. Four brighter regions can be pinpointed at first sight, most likely related to the four wells. Hence, neurons within the wells would constitute the main modules of the network.

A more exhaustive analysis, though, unveils a fifth faint community between the others: it corresponds to the middle of the PDMS mold, where some neurons also grew, behaving as a bridge connecting the four main communities. From this weak structural attachment arises a rich functional relation between modules, which is pointed out by non-null values out of the diagonal of the connectivity matrix. This specific feature is also observed in [2] and ratified by an outstanding $\Theta \simeq 0.21$, the highest of our studied cultures.

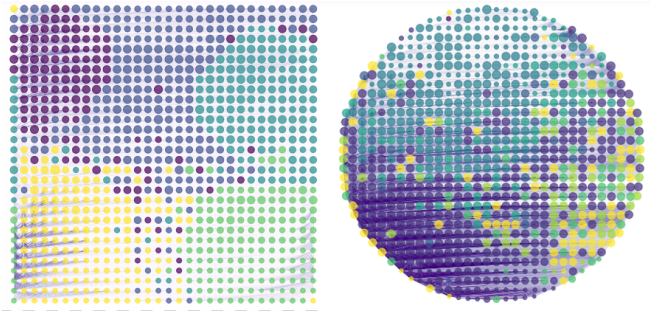

FIG. 4: Community louvain algorithm applied to our cultures using the Brain Connectivity Toolbox and plotted with NetworkX. Appart from weighted links, nodes are also weighted considering closeness, betweness and eigenvector centrality. Note that in the PDMS culture two main communities can be distinguished, very likely relatable to the pinpointed modules in the TE adjacency matrix.

C. A culture in an embossed PDMS surface

To complete the picture, a third experiment was added to our pipeline. Recorded at 100 fps during approximately 180 seconds, this culture was grown in a PDMS mold with a subtly embossed surface. This relief was sufficient to slightly direct the creation of new synapses between neurons while keeping a certain homogeneity in the culture.

The first thing that should call our attention is a major change in the main attributes of the raster plot (Fig. 2C, column I) . Even though the average IBI is not far from that of the previous cultures, what is surely to be remarked is what we see at the bottom-left corner of the raster plot. Here, firings do not occur as coherent episodes ('columns' of activity in the raster), but a slower propagation of the impulses seems to occur: a completely different state of the system from the ones we had previously studied.

A visualization of the recordings helps us to relate these brand new activity patterns to waves of firings, emerging from sundry regions and spreading at different speeds. We can also observe that the subsequent episodes of coherent bursts display an oscillatory character too, yet with a more rapid transmission.

A second quality of this culture that can be seen in the raster is the depletion in the number of neurons involved in GNAs along time. This fact becomes apparent when

the GNAs distribution is plotted (Fig. 2C, column II): a *pdf* distinctly shifted to the left and peaked at a poor 10% of the culture's ROIs is what we obtain.

The aspect of the correlation coefficients' distribution is also intriguing: despite some gaps at higher values and the ones below the calculated noise threshold, a rather flat histogram emerges. Hence, the associated functional complexity goes up to $\Theta_{\mathrm{CC}} \simeq 0.52$, which can be multiplied by $\Theta_{\mathrm{GNA}} \simeq 0.31$ to get a Dynamical Richness of the culture $\Theta \simeq 0.16$. Note that the narrow variability in GNA sizes discussed above exerts a substantial influence on the lowering of the latest value calculated.

As an initial probe of the cultures' functional connectivity, the adjacency matrix calculated from crossed correlation values is also plotted in Fig. 2C, column III. A quite large section of the graphic seems to be closely correlated, but its border cannot be easily delimited as it gradually fades.

To shed some light on the previous issue, the TE connectivity matrix comes off as an improvement of the former (Fig. 2C, column IV), as two modules can be clearly identified at the top of the diagonal and which could perhaps be related to a couple of recurrent nucleation zones in our culture also seen in Fig. 4. But then, there is this big, weakly defined module at the bottom-right corner, the firings within which are saddled between a notably coherent state and a non-correlated one.

Moreover, a relatively high number of connections are present outside the diagonal of the matrix, indicating that the different modules are well connected among themselves, thus there exists a strong level of communication among distinct parts of the culture. Indeed, a noteworthy global efficiency of $G_{\mathrm{EFF}} \simeq 0.84$ underpins this hypothesis.

TE analysis provides a modularity of $\mathcal{Q} \simeq 0.33$, since the two aforementioned modules contribute significantly to raise it. When it turns to CC analysis, however, a non realistic and extremely low $\mathcal{Q} \simeq 0.05$ is obtained.

In general, TE-based methods provide higher values of the parameter than those from CC, specially when the Z score is increased (as we should expect given its definition, see Materials and Methods). This bias of the CC method comes not as a surprise, as networks appear more connected than what they actually are when connectivity diagrams are plotted using CC values as link weights.

V. CONCLUSIONS

Some final remarks can be elaborated regarding the obtained results and their interpretation.

Firstly, *in vitro* techniques have proved to provide a new insight when trying to understand the relation established between structural and functional connectivity of neuronal networks. Unlike MRI or other similar approaches, this way of proceeding enables us to track with a stunning spatiotemporal resolution both single cell and culture-level activity patterns.

Furthermore, since we wiped the slate clean by allowing synapses to freely emerge again, our cultures do not display any kind of 'structural memory'. Hence, the effects of the introduced perturbations on the molds' reliefs can be unshieldedly observed and quantified. For instance, some variations caused by the obstacles could be perceived in the propagation directions and timescales characterizing the electrical impulses.

We could also corroborate that rather weakly connected cultures exhibit a broader range of possible dynamical states, as seen in Refs. [1] and [2]. Even though the dynamical richness increases in these circuits, it is not at expense of a substantial fall in G_{EFF}, which is maintained considerably high. Therefore, cultures with the aforementioned structural features will most likely be the ones able to support functionally complex processes similar to those performed by natural neuronal networks.

All in all, we hope that this study has contributed, even just by a little, to pave the way towards a better understanding of one of the most fascinating and poorly understood networks: the brain.

Acknowledgments

I would like to gratefully thank my advisor, Dr. Jordi Soriano, for giving me the opportunity to see the tip of the iceberg of this fascinating field of study, for his wise pieces of advise and endless patience. I would also like to thank Carla, Miquel and Guillermo, as first steps in an unknown field are always easier to take if they are shared. Finally, this work wouldn't have reached to an end if it weren't for the unconditional support of my parents.

[1] S. Okujeni et al., *Mesoscale Architecture Shapes Initiation and Richness of Spontaneous Network Activity*, Journal of Neuroscience 5 April 2017, 37 (14) 3972-3987

[2] H. Yamamoto et al., *Impact of modular organization on dynamical richness in cortical networks.* Sci. Adv. **4** , eaau4914 (2018).

[3] J. Orlandi et al., *Noise focusing and the emergence of coherent activity in neuronal cultures.* Nature Phys **9**, 582–590 (2013).

[4] J.G. Orlandi et al., *NETCAL: An interactive platform for large-scale, network and population dynamics analysis of calcium imaging recordings*, Zenodo (2017).

[5] G. Zamora-López et al., *Functional complexity emerging from anatomical constraints in the brain: The significance of network modularity and rich-clubs.* Sci. Rep. 6, 38424 (2016)

[6] M. Rubinov, O. Sporns, *Complex network measures of brain connectivity: Uses and interpretations.* Neuroimage **52**, 1059-1069 (2010).